ELSEVIER

Biophysical Chemistry 63 (1997) 167–183

Biophysical Chemistry

Chaos in a minimal model of the alternative pathway of the complement system

Enrique Peacock-López [a,*], Katherine L. Queeney [b,1]

[a] *Institute of Theoretical Dynamics, University of California Davis, Davis, CA 95616 USA*
[b] *Department of Chemistry, Williams College, Williamstown, MA 01267 USA*

Received 28 June 1996; accepted 31 July 1996

Abstract

In previous work, we introduced a minimal model of the alternative pathway of the complement. We also limited our analysis to a reduced set of parameter values because, for some parameters, experimentally supported estimates were not found. On the other hand, changes in value of some parameters may be a result of a pathological condition. Therefore, here we extend our analysis and include a wider range of values of five of the physiologically relevant parameters. For all the parameters considered, we observe chaotic oscillations, and we construct bifurcation diagrams using Poincaré sections of local maxima.

Keywords: Alternative pathway; Chaos; Complement system; Minimal model

1. Introduction

An enzyme cascade is defined [1] as any sequential array of enzymatic reactions in which the product of one reaction acts as the catalyst for the next reaction. The evolution of this type of mechanism, with its typically complex regulation, can be characterized by the types of stimuli to which enzyme cascades respond. As part of the humoral immune system, a group of plasma and cell membrane proteins forms the complement system. The complement system is an enzyme cascade [2,3]. The complement proteins mediate processes such as inflammation, neutralization of pathogens, clearance of immune complexes and cell membrane disruption. A multistep mechanism is involved that is quite complex, but only two initiation pathways can lead to the activation of complement response. For human and murine complement proteins, experimental biochemical studies have yielded a wealth of structural and mechanistic information about this complex system of enzyme cascading processes [4,5]. Previous analyses of the kinetics of complement [6,7] have provided a general picture of the overall behavior of the system. However, the approximations required to make such an analysis mathematically feasible necessarily obscure much of the fine detail of the kinetic behavior of individual components of the system.

In previous work [8,11], we have studied the

* Corresponding author.
[1] Present address: Department of Chemistry, Harvard University, Cambridge, MA 02138, USA.

PII S0301-4622(96)02213-2

kinetics of the so-called alternative pathway. For this pathway, including sources of infection and an adjustable supply of the initial C3 protein, a minimal model has been constructed. Rate constants for the model have been estimated from reported data, and the ordinary differential equations associated with the model have been analyzed by numerical integration [10,12]. This minimal model exhibits sustained oscillatory behavior. Such behavior is expected from a complex biochemical system with the feedback characteristics of the alternative pathway. Moreover, if we vary the deactivation parameter, we find that the oscillations undergo period doubling [8,9].

Our minimal model of the alternative pathway of complement represents the first modeling work of this kind performed on this system. That a model designed directly from an actual biochemical mechanism, and described by experimentally obtained parameters, exhibits oscillatory behavior strongly suggests that such behavior may be a legitimate part of this system. Because of its relative shortage of complex individual steps, this is one of the simplest models for which such behavior has been observed. Considering the relative simplicity of the model, which includes only two bimolecular steps and a first order autocatalytic step, the model has shown a dynamic complexity never seen before in other theoretical analyses of the complement [13,14]. Also, the appearance of period doubling [9] opens up the possibility of more complex dynamics and chaotic behavior in the system. Ultimately, we hope that studies such as this will lead to experimental research to verify the existence of the time behavior our model predicts. For example, periodic measurements of the pivotal C3 protein concentration will test our theoretical predictions.

In our approach we construct models of biochemical systems by determining the mechanisms and fundamental steps that characterize them. We apply the laws of mass action to the chemical species represented in the mechanism to construct a set of ordinary differential equations (ODEs). The differential equations are integrated numerically [15] and the concentrations are plotted against time. Also, two-dimensional plots of the concentration of two different species over a period of time allow for the characterization of the system and the identification of various types of behavior ranging from steady states to chaos.

To study in detail the kinetics of the different component concentrations of the complement as they behave under the influence of the entire system, we have proposed a minimal model (QPL) derived from the accepted mechanism of the cascade [9]. A full explanation of the QPL model and the underlying biochemistry has been discussed elsewhere [8,11]. The mechanism is itself derived from experimental studies; simulations derived from this mechanism permit elucidation of the behavior that may be masked by experimental conditions or the simplifications of previous kinetic analyses. In our work, we have characterized the minimal model both qualitatively and quantitatively. Our preliminary results [8,9] have shown that complex behavior can be achieved if the parameters, originally calculated from reported experiments, are varied within plausible physical bounds. Further characterization of the parameter space is necessary; so too is that of the implications to the biochemical mechanism [16–25] and experimental observation.

In Section 2 we review the minimal model of the alternative pathway of complement. In Section 3, we consider the time series obtained from the numerical integration of the system of ODEs associated with the minimal model. We follow, in Section 4, with the construction of Poincaré sections defined for maxima of the concentrations for parameters within physical bounds. Finally, in Section 5 we discuss our results.

2. Minimal model of the alternative pathway

Complement is a series of well characterized interacting proteins that comprise one arm of the immune system. The system is activated in a cascade fashion in response to the presence of antibodies or foreign cells. There are two distinct pathways which lead to the full activation of the complement system: the classical and the alternative. The pathways are distinct in the method of activation and in some of the component proteins involved. However, the pathways converge around the C3 protein and are identical in the final result: the formation of the membrane attack complex (MAC) and the death of the targeted cell. Both pathways are depicted in Fig. 1. As in many biochemical mechanisms [19,20], the alterna-

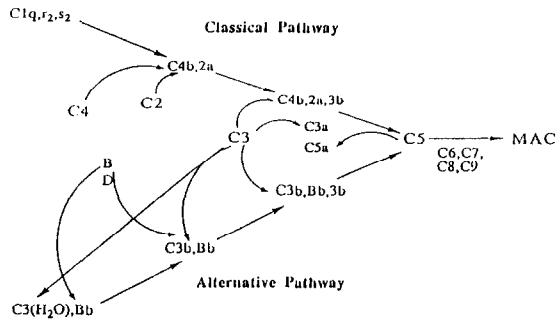

Fig. 1. Simplified diagram of complement mechanism.

tive pathway is regulated and controlled; either activation or inactivation at the wrong time is extremely dangerous.

The mechanism of the alternative pathway is depicted in Fig. 2. Central to the alternative pathway is the C3 protein, which will be referred to as A. Concentration of this protein in blood is monitored by the liver. Also, the protein is not reactive but is easily hydrolyzed. The hydrolyzed form, B2, is highly reactive and is the first step in the pathway. Thus we model these processes with the following mechanistic step

$$(A - A_0) \xrightarrow{k_0} A \xrightarrow{k_1} B2 \tag{1}$$

The next step involves the highly reactive B2 and other cofactors, which are in excess. The end product yields a C3 convertase, referred to here as E1

$$B2 \underset{k_{d1}^-}{\overset{k_{d1}^+}{\rightleftharpoons}} E1 \tag{2}$$

The convertase catalyzes the formation of another reactive protein, C3b, which is denoted by Ab. The mechanistic step is depicted by following equation

$$A + E1 \underset{k_{E1}^-}{\overset{k_{E1}^+}{\rightleftharpoons}} C_1 \xrightarrow{k_{E1}} E1 + Ab \tag{3}$$

where we have assumed a Michaelis–Menten mechanism with an intermediate C1.

The product Ab is involved in several possible reactions. It could bind with the same cofactors used by B2 and form a second form of a C3 convertase. Although structurally different, B2 and Ab are mechanistically similar. Thus we model this property as

$$Ab \xrightarrow{k_2} B2 \tag{4}$$

Notice that this is an amplification loop, as the product will generate more catalyst which in turn will generate more product. The second role of Ab is to attach to cell membranes, forming C5 convertase and the MAC. Eventually, the invading organism gets destroyed and the process stimulates the formation of more C3. In this case we have contracted several mechanistic steps into

$$Ab + Z \xrightarrow{k_{0A}} A + Ab \tag{5}$$

Although B2 and Ab are reactive, they can also bind to inhibiting factors, yielding an inactive species. The inhibition of these two components is modeled as

$$B2 \xrightarrow{k_{d1}} I_1 \tag{6}$$

$$Ab \xrightarrow{k_{d1}} I_2, \tag{7}$$

where we have assumed that the inhibitor factors are in excess and assigned the same rate constant k_{d1}. Finally, we consider that the invader specied is injected into the system

$$Inf \xrightarrow{k_{inf}} Z \tag{8}$$

and it reproduces

$$Z \xrightarrow{k_{rep}} 2Z \tag{9}$$

Thus Eqs. (1)–(9) constitute the minimal model of the alternative pathway of the complement sys-

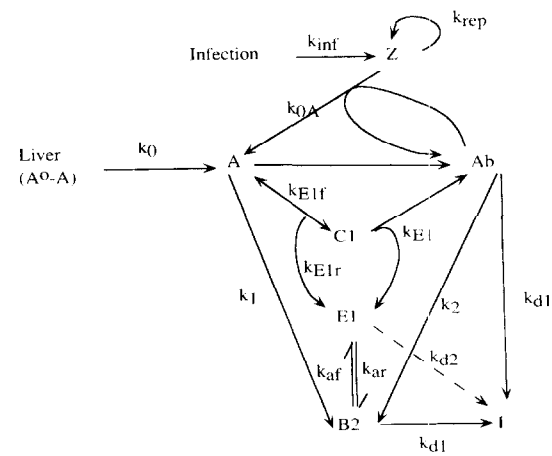

Fig. 2. Schematic diagram of the minimal model of the alternative pathway.

tem. It models the role of C3 in the initiation of the complement response and contracts the steps involving the MAC. Thus we have modeled in more detail the initiation and the amplification of the alternative pathway of the complement response.

3. Numerical results

The minimal model of the activation of the alternative pathway of the complement system is analyzed by numerical integration of the ODEs associated to the mechanism. From Eqs. (1)–(9) and applying the mass action laws, we obtain the following set of ODES

$$\frac{dZ}{dt} = k_{rep}Z + k_{inf} - k_{0A}Z\,Ab \tag{10}$$

$$\frac{dA}{dt} = k_0(A_0 - A) + k_{0A}Z\,Ab + k_{E1}^{-}C1 - k_1 A - k_{E1}^{+}A\,E1 \tag{11}$$

$$\frac{dB2}{dt} = k_1 A + k_2 Ab + k_{a_1}^{-}E1 - k_{a_1}^{+}B2 - k_{d1}B2 \tag{12}$$

$$\frac{dC1}{dt} = k_{E1}^{+}A\,E1 - k_{E1}^{-}C1 - k_{E1}C1 \tag{13}$$

$$\frac{dE1}{dt} = k_{E1}^{-}C1 + k_{E1}C1 + k_{a_1}^{+}B2 - k_{a_1}^{-}E1 - k_{E1}^{+}A\,E1 \tag{14}$$

$$\frac{dAb}{dt} = k_{E1}C1 - k_2 Ab - k_{d1}Ab \tag{15}$$

Notice that this set of ODEs has only two second order terms, and the autocatalytic step is first order.

Table 1

Parameter	Value
$[A]_0$	7.2×10^{-6} M
k_1	0.003 h^{-1}
k_2	1.0×10^{6} h^{-1}
k_{a1}^{+}	10.0 h^{-1}
k_{a1}^{-}	36.0 h^{-1}
k_{E1}	7.2×10^{6} h^{-1}
k_{E1}^{+}	3.6×10^{12} M^{-1} h^{-1}
k_{E1}^{-}	3.6×10^{10} h^{-1}

Table 2

Parameter	Value
k_0	0.1 h^{-1}
k_{0A}	1.0×10^{11} M^{-1} h^{-1}
k_{inf}	1.31×10^{-6} M h^{-1}
k_{rep}	1.0 h^{-1}
k_{d1}	bifurcation parameter/h^{-1}

The set of ODEs defined by Eqs. (10)–(15) has been analyzed using the packages PLOD [12] and INSITE [10]. Some parameters were estimated in previous work [8,11]. In contrast with our previous work [9], we will allow some variations in parameter values. Some parameters needed in the computational analysis are better defined from the literature than others. For example, values of eight parameters are shown in Table 1. Also, parameter values in Table 2 correspond to typical values used in our computations. However, these parameters either are not well defined from the literature or may be related to physiological variation. Once the parameters are selected, the set of ODEs can be integrated using PLOD's [12] implementation of the Gear [15] algorithm with accuracy ranging between 10^{-10} and 10^{-12}. On the other hand, INSITE allows us to study the behavior of the system as we vary the value of a particular parameter. Namely, we calculated the Poincare sections for five of the system parameters.

For example, Tables 1 and 2 contain parameters similar to the values used in our previous work [9]. For these parameters Fig. 3 depicts a Poincaré sec-

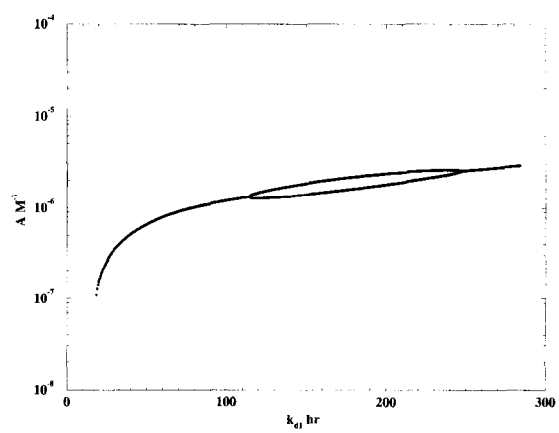

Fig. 3. Poincaré section defined by the maximum of [A], varying k_{d1} and all other parameters given in Table 1 and Table 2.

Table 3

Parameter	Value
$[A]_0$	7.2×10^{-6} M
k_1	0.003 h^{-1}
k_2	1.0×10^{6} h^{-1}
k_{d1}^{+}	10.8 h^{-1}
k_{d1}^{-}	36.0 h^{-1}
k_{E1}	7.2×10^{6} h^{-1}
k_{E1}^{+}	3.6×10^{12} M^{-1} h^{-1}
k_{E1}^{-}	3.6×10^{10} h^{-1}

Table 4

Parameter	Value
k_0	0.1 h^{-1}
k_{0A}	1.0×10^{11} M^{-1} h^{-1}
k_{inf}	1.27×10^{-6} M h^{-1}
k_{rep}	1.0 h^{-1}
k_{d1}	285 h^{-1}

tion for the maximum value of the concentration of A, with bifurcation parameter k_{d1}. This result is consistent with our previous observation [8,9] of period doubling in the minimal model.

Although we want to consider a wider range of parameter values, we also want to stay within physically relevant bounds. For example, we estimate k_{inf} from other experiments. In the case of glycolytic oscillations, glucose is pumped into the system at rates varying from 36 to 150 mM h^{-1}. Thus, we considered in Table 4 (below) a value roughly three orders of magnitude smaller than the maximum pumping rate used in glycolytic oscillations.

For the values in Tables 3 and 4, we observe complex oscillations in the concentrations. For example, Figs. 4 and 5 depict the time behavior of the concentration of the six variables. Certain similarities in shape between [C1] and [Ab] and between [B2] and [E1] are noticeable. Also, Fig. 6 depicts one oscillation for the concentration of A as a function of time. Fig. 7 shows its corresponding phase plot of [A] vs. [Z], and Fig. 8 depicts the phase plot of [Z] vs. [Ab]. Fig. 9 depicts the attractor's three-dimensional, (A, Ab, Z), projection. Notice the differences between the maxima and the minima. These differences range between eight and thirteen orders of magnitude. This behavior simply reflects the stiffness of the differential equations.

Now,if we make some minor changes in k_{inf}, we observe more complex dynamics. Figs. 10–14 were

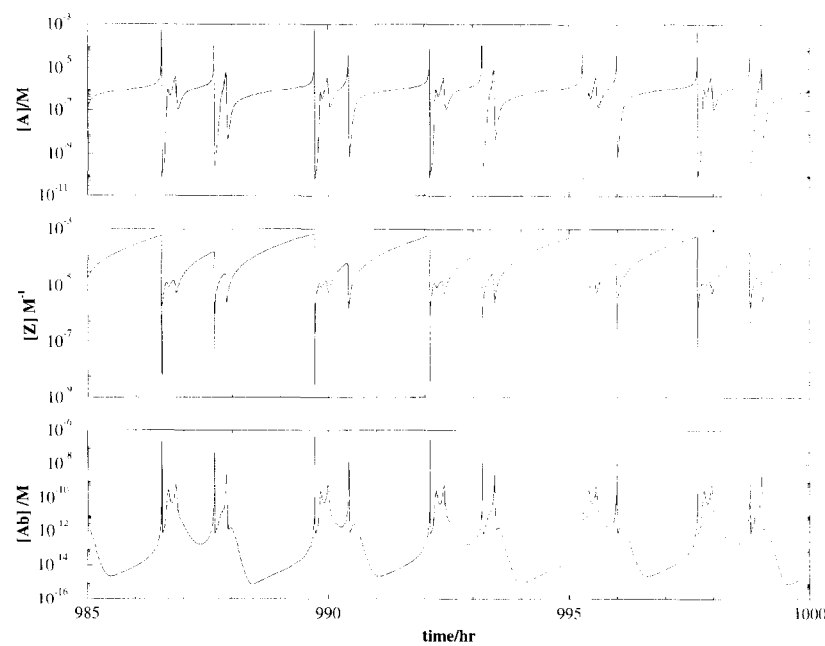

Fig. 4. Concentration vs. time plots for A, Z, and Ab. Parameters were taken from Table 3 and Table 4.

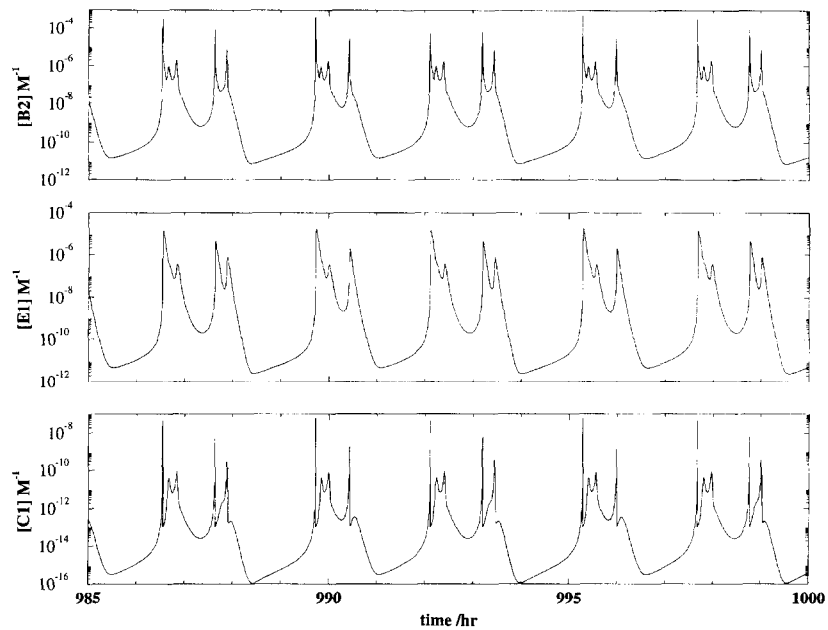

Fig. 5. Concentration vs. time plots for B2, E1 and C1. Parameters were taken from Table 3 and Table 4.

generated with the parameter values in Tables 3 and 5. The time series depicted in Fig. 10 shows aperiodic behavior and can be compared with Fig. 4. Fig. 11 blows up some of the features of the behavior of A, which can be compared with Fig. 6. Figs. 7 and 8 can be compared with Figs. 12 and 13, which are phase portraits with their corresponding magnification. Finally, Fig. 14 depicts the attractor's three-dimensional projection. This figure can be compared with the attractor's projection in Fig. 9.

Tables 1 and 6 differ slightly from Tables 3 and 5 and the time series also show small differences. Fig. 15 shows the (Z, A) and the (Z, Ab) phase portraits. Also, Fig. 16 shows all the 15 possible phase portraits. Notice the (C1,E1) portrait. It appears to be a linear relationship between the C1 and the E1 species.

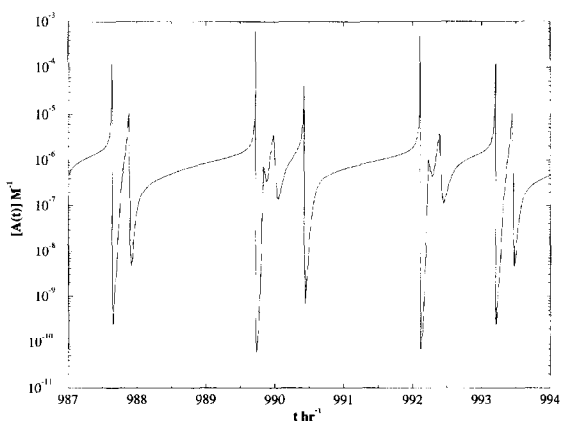

Fig. 6. Amplification of an oscillation of [A]. Parameters were taken from Table 3 and Table 4.

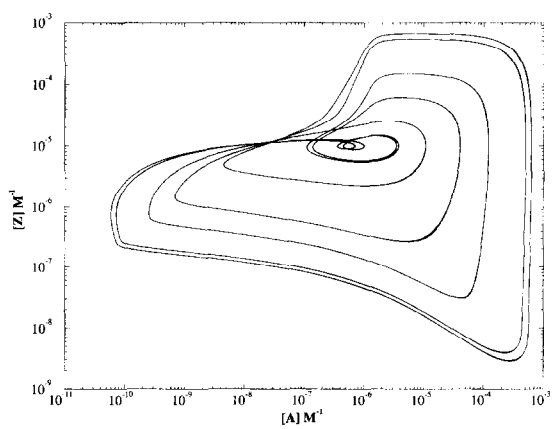

Fig. 7. Phase plane [Z] vs. [A] for sustained oscillations in the minimal model with parameters taken from Table 3 and Table 4.

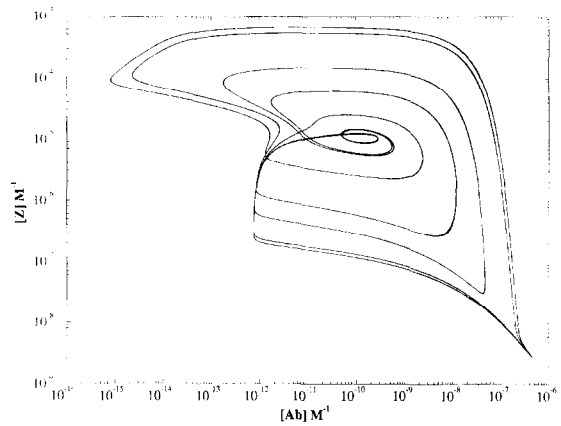

Fig. 8. Phase plane [Z] vs. [Ab] for sustained oscillations in the minimal model with parameters taken from Table 3 and Table 4.

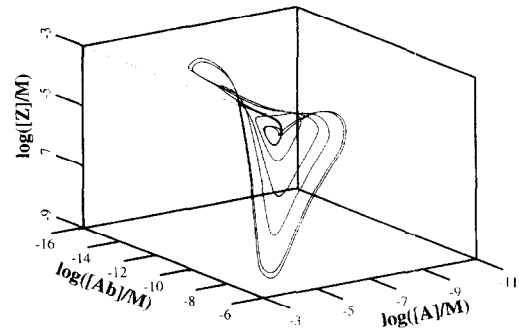

Fig. 9. Three-dimensional (A, Ab, Z) projection of the six-dimensional attractor for parameters in Table 3 and Table 4.

Finally, Fig. 17 shows the three-dimensional (A, Ab, Z), projection of the six-dimensional attractor.

The time series of the numerical solutions of the ODEs associated with the minimal model shows complex behavior. We have obtained both complex oscillation and chaotic behavior. Thus the minimal model of the alternative pathway shows complex dynamics even though it has only two second-order nonlinearities and only one autocatalytic step of order one. Finally, notice that the concentration values are within physical bounds.

4. Bifurcation diagrams

As we want to explore a wider range of parameter values, we consider in this section the bifurcation diagrams associated with the QPL model. The bifurcation diagrams are calculated using Poincaré sec-

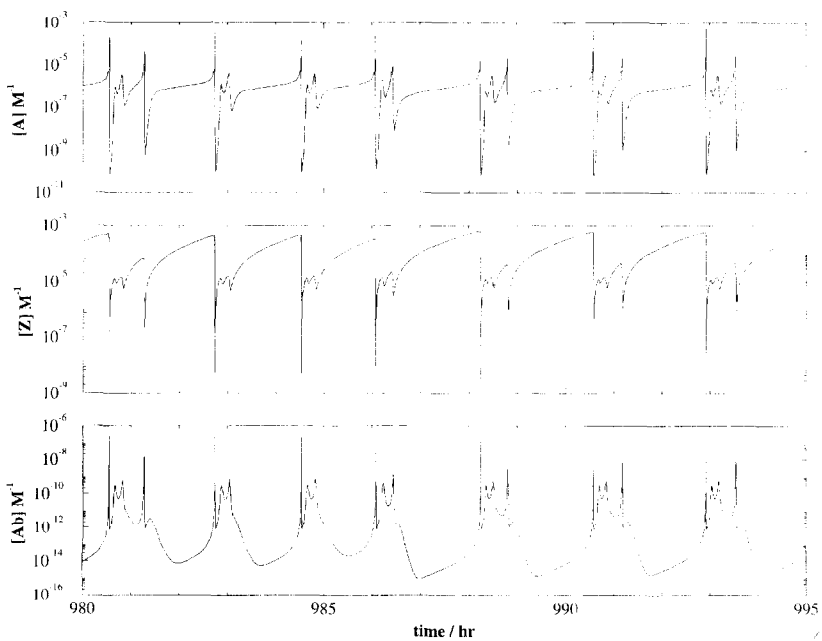

Fig. 10. Concentration vs. time plots for A, Z, and Ab. Parameters were taken from Table 3 and Table 5.

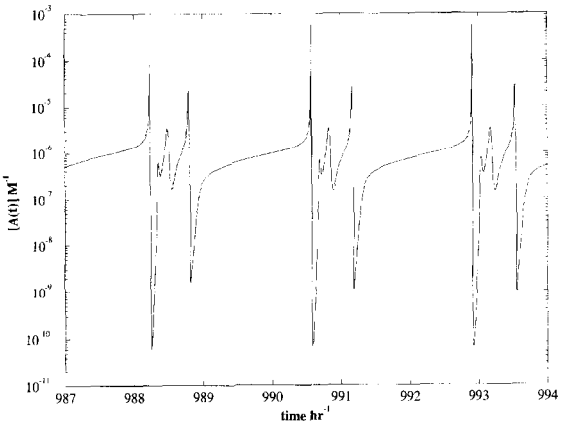

Fig. 11. Amplification of an oscillation of [A]. Parameters were taken from Table 3 and Table 5.

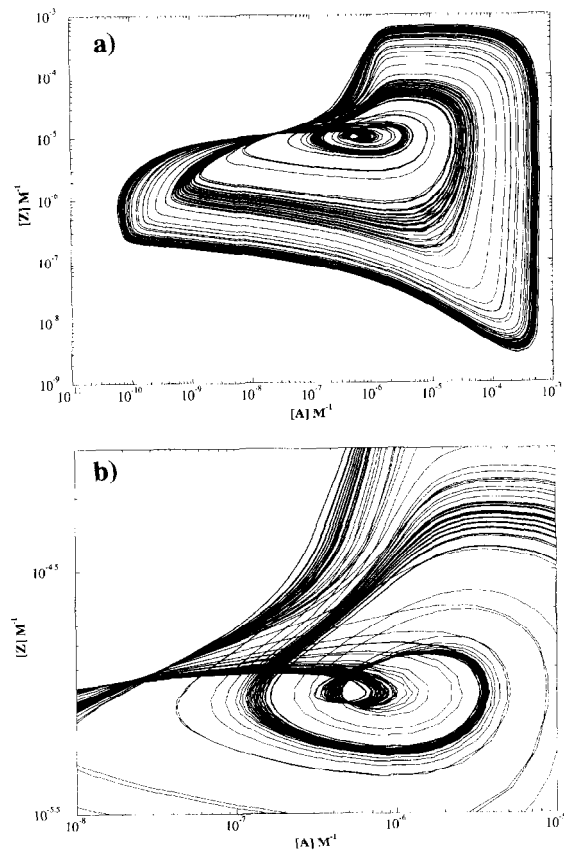

Fig. 12. (a) Phase plane [Z] vs. [A] for aperiodic oscillations in the minimal model with parameters taken from Table 3 and Table 5; (b) amplification of the phase plane.

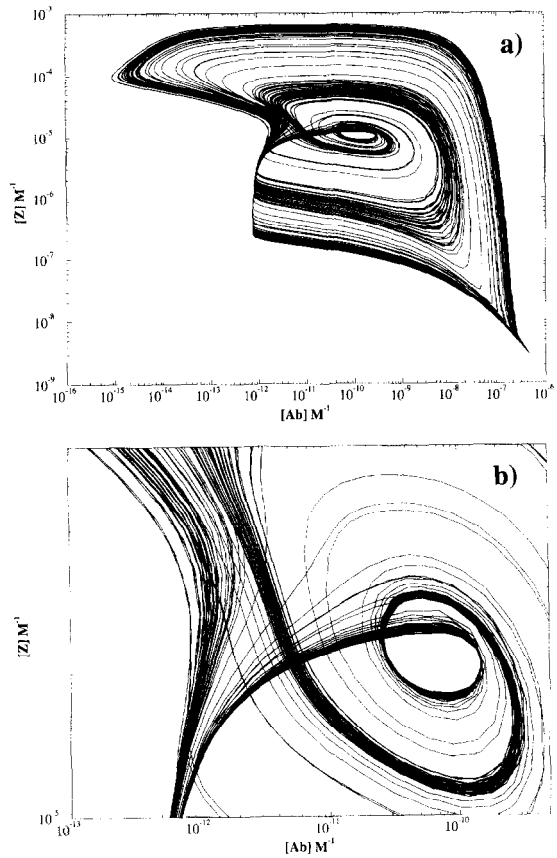

Fig. 13. (a) Phase plane [Z] vs. [Ab] for aperiodic oscillations in the minimal model with parameters taken from Table 3 and Table 5; (b) amplification of the phase plane.

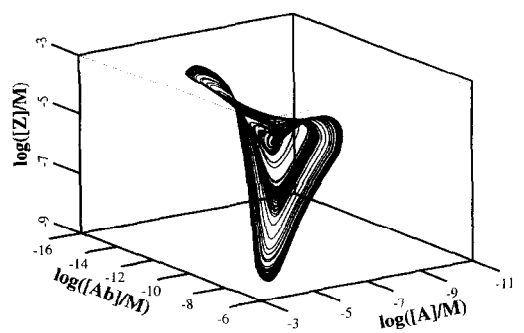

Fig. 14. Three-dimensional (A, Ab, Z) projection of the six-dimensional attractor for parameters in Table 3 and Table 5.

Table 5

Parameter	Value
k_0	$0.1\ h^{-1}$
k_{0A}	$1.0\times10^{11}\ M^{-1}\ h^{-1}$
k_{inf}	$1.31\times10^{-4}\ M\ h^{-1}$
k_{rep}	$1.0\ h^{-1}$
k_{d1}	$285\ h^{-1}$

tions of the local maxima. This diagrams will allow us to study the dynamics in parameter space. Again we will consider values within physical bounds and assigned different parameters as bifurcation parameter.

4.1. k_{d1}

One of the most significative parameters is k_{d1}. As this parameter is related to the sytems' capacity to inhibit the complement's reactive species C3(H_2O) and C3b, any change in this parameter is important and may be related to factor I and/or other cofactors. The changes in k_{d1}^{+} may be due to variations in the inhibitor concentrations. These changes could be traced back to protein expression, and perhaps related to pathological conditions.

First we considered parameters from Tables 1 and 5, with k_{d1} as the bifurcation parameter. Figs. 18 and 19 show the Poincaré section for the maximum value of the corresponding concentrations ([A], [Z]), for values of k_{d1} up to $500\ h^{-1}$. Fig. 20 depicts the same Poincaré section but now for values of k_{d1} up to $3000\ h^{-1}$, and Fig. 21 shows the section for values up to $7000\ h^{-1}$. Finally, Fig. 22 blows up the region around $2000\ h^{-1}$ and shows in more detail the structure of the bifurcation diagram.

Next we only change the rate of replication k_{rep} to $3\ h^{-1}$, which should be the upper bound for this parameter. The net effect of this change is to increase the rate of reproduction of the invading species. The consequence of this change is depicted in Fig. 23 for values of k_{d1} below $500\ h^{-1}$. Fig. 24 expands the region of values of k_{d1} up to $3500\ h^{-1}$ and Fig. 25 shows that up to $10000\ h^{-1}$. If we compare Fig. 21 with Fig. 25, we notice that the net effect of the changing k_{rep} is to enlarge the chaotic region and increase the number of maxima from two to six in the region of large values of k_{d1}. In order to look in more detail at the bifurcation diagram, we have blown up the regions from 0 to $1750\ h^{-1}$ and from 1750 to $3550\ h^{-1}$ in Fig. 26. In Fig. 27 we depict the region between 1250 and $1750\ h^{-1}$, which shows even finer details of the bifurcation diagram. For example, in Fig. 27(a), we consider values of [A]

Table 6

Parameter	Value
k_0	$0.1\ h^{-1}$
k_{0A}	$1.0\times10^{11}\ M^{-1}\ h^{-1}$
k_{inf}	$1.29\times10^{-4}\ M\ h^{-1}$
k_{rep}	$1.0\ h^{-1}$
k_{d1}	$192\ h^{-1}$

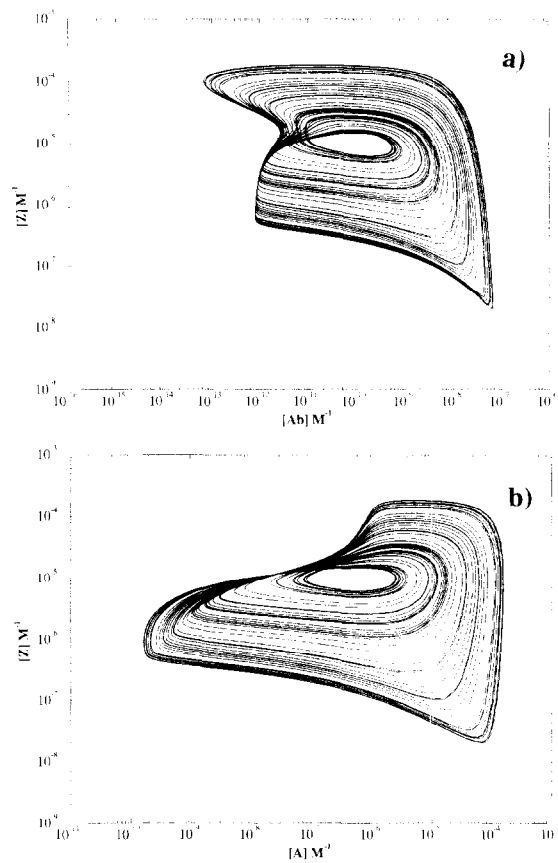

Fig. 15. (a) Phase plane [Z] vs. [Ab]; (b) phase plane [Z] vs. [A], for aperiodic oscillations in the minimal model with parameters taken from Table 3 and Table 6.

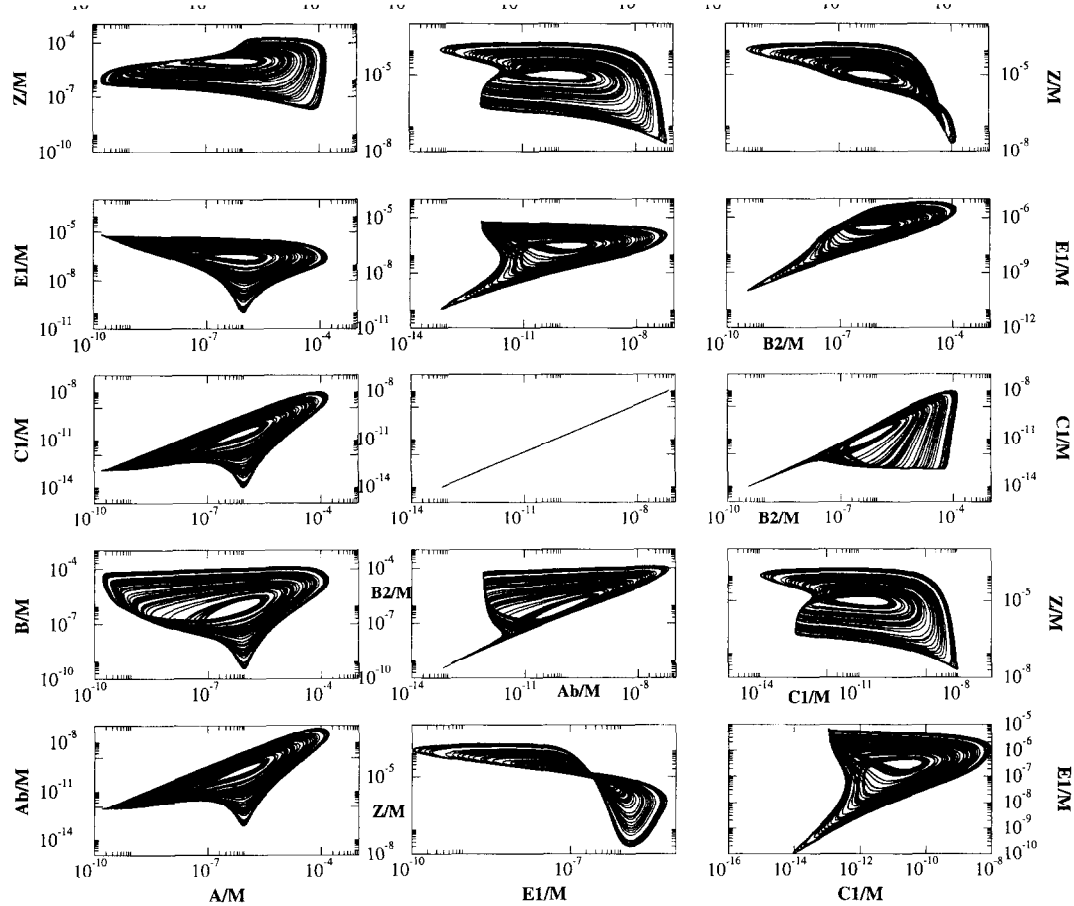

Fig. 16. All possible phase planes for aperiodic oscillations in the minimal model with parameters taken from Table 3 and Table 5.

between 10^{-8} M and 10^{-3} M. Moreover, in Fig. 27(b) we magnify the upper region in the concentration of A, e.g., [A] $\in [5 \times 10^{-6}, 3 \times 10^{-4}]$. Finally, in Fig. 27(c) we consider values of [A] between 10^{-8} and 10^{-6} M. Notice that for values of k_{d1} around approximately 1415, we could observe complex oscillations with 20 maxima.

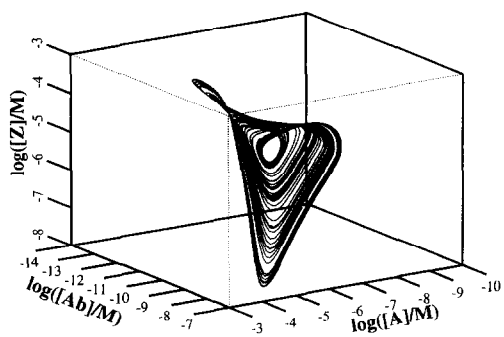

Fig. 17. Three-dimensional (A, Ab, Z) projection of the six-dimensional attractor for parameters in Table 3 and Table 6.

As the third and final change, we considered a small k_{rep} equal to 0.3 h^{-1}. In this case we have slowed down the rate of reproduction. Fig. 28 depicts the diagram for values of k_{d1} up to 500 h^{-1}. In this figure we can notice the contraction of the chaotic region, yielding more regular oscillations.

In summary, we observe that the behavior of the system tends to a larger chaotic region in k_{d1} as the rate of reproduction of the offending species increases.

4.2. Other parameters

Another four parameters are considered in this work. First we look at the influx rate of Z, which can

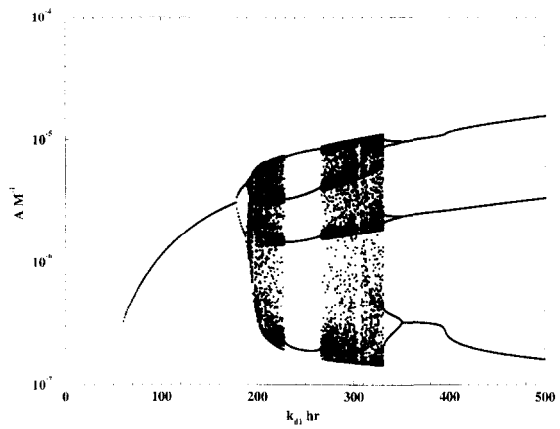

Fig. 18. Bifurcation diagram of A calculated using Poincaré sections of local maxima. Parameter were taken from Table 1 and Table 5; k_{d1} is the bifurcation parameter.

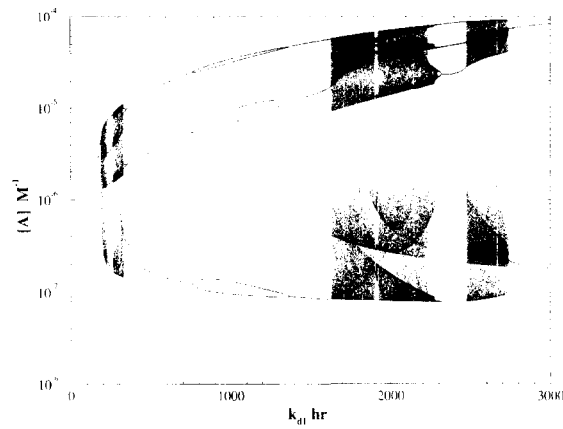

Fig. 20. Bifurcation diagram of [A] calculated using Poincaré sections of local maxima. Parameter were taken from Table 1 and Table 5; k_{d1}, the bifurcation parameter, varying from zero to 3000 h^{-1}.

be estimated from other experimental work such as the case of oscillation in glycolysis. Next we consider the response of the liver to changes in the concentration of C3. This term is similar to a CSTR term in the case of chemical systems. Third, we chose the rate of duplication of the invading species, as this seems to have an important effect in the bifurcation diagrams of the inhibition step. Finally, we consider the most contracted part of the model, which characterized the MAC attack and destruction of the foreign agents or "non-self".

4.2.1. k_{inf}

An estimated parameter is the influx rate of an offending species, k_{inf}. Using as a reference the rates of injection of glucose in glycolytic oscillations [26], we consider a range of values for k_{inf} between 0.05 and 0.20 mM h^{-1}; other parameters were taken from from Tables 1 and 5. Using k_{inf} as the bifurcation parameter, Fig. 29 depicts regions of chaotic behavior and regions of regular oscillations. Also, Fig. 30 shows the period doubling route to chaos.

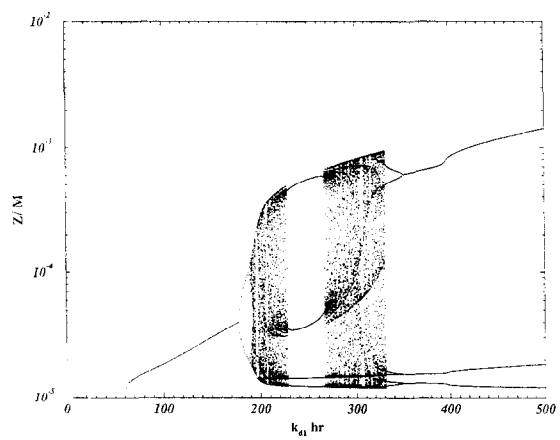

Fig. 19. Bifurcation diagram of [A] calculated using Poincaré sections of local maxima. Parameters were taken from Table 1 and Table 5; k_{d1}, the bifurcation parameter, varying from zero to 500 h^{-1}.

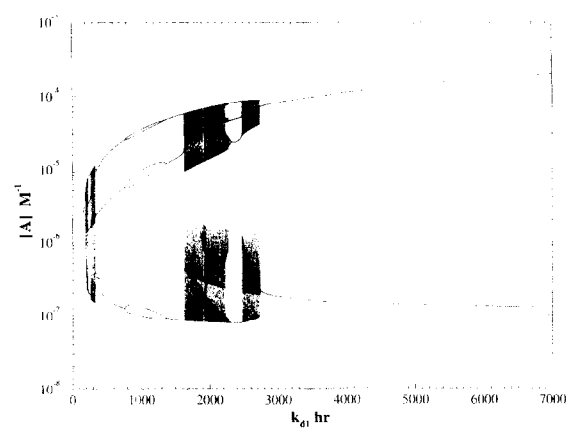

Fig. 21. Bifurcation diagram of [A] calculated using Poincaré sections of local maxima. Parameters were taken from Table 1 and Table 5; k_{d1}, the bifurcation parameter, varying from zero to 7000 h^{-1}.

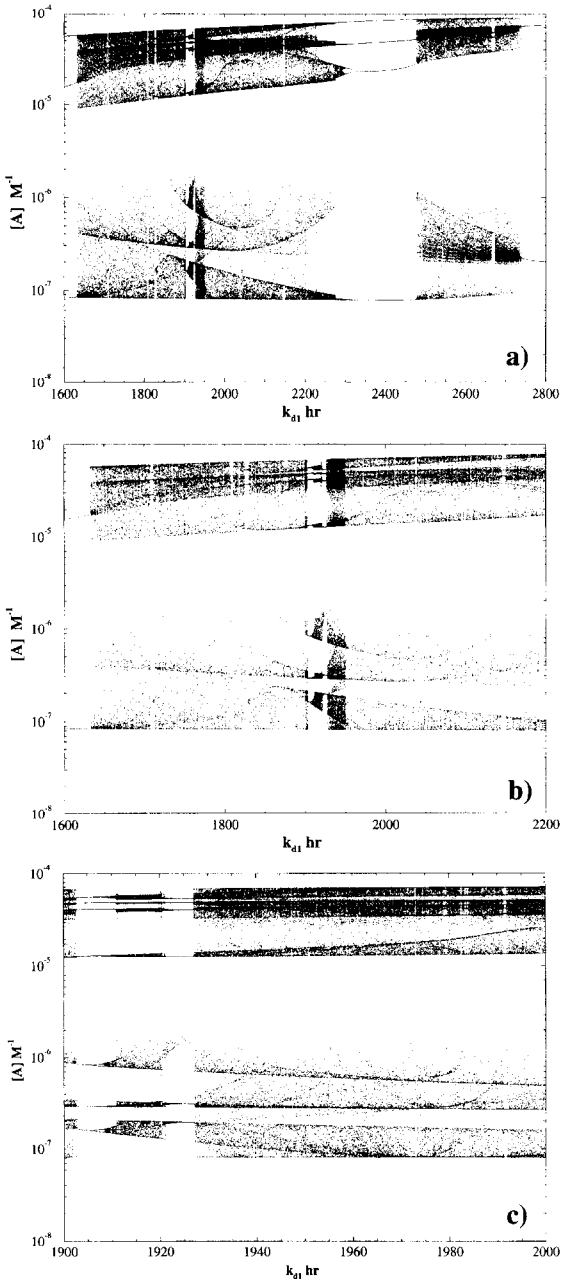

Fig. 22. Amplifications of Fig. 2O: (a) k_{d1} hr $\in$[1600, 2800]; (b) k_{d1} h $\in$[1600, 2200]; (c) k_{d1} h $\in$[1900, 2000].

For k_{inf} we observe periodic oscillations for the largest and the smallest of the values. For intermediate values, we observe the period doubling route to chaos.

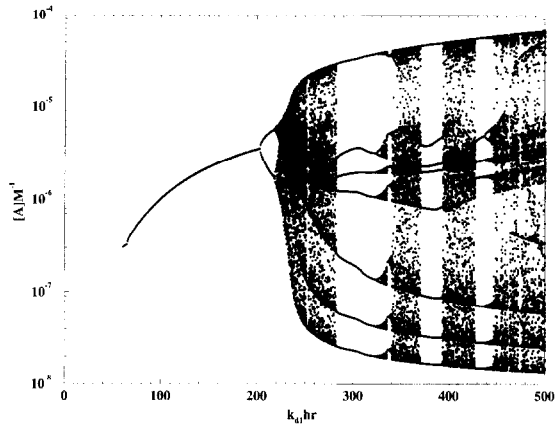

Fig. 23. Bifurcation diagram of [A] calculated using Poincaré sections of local maxima. Parameters were taken from Table 1 and Table 5 with $k_{rep} = 3.0\ h^{-1}$ and k_{d1}, the bifurcation parameter, varying from zero to 500 h^{-1}.

4.2.2. k_0

The response of the liver to changes in the concentration of C3 (A) is not well documented, but physical upper and lower bounds can be considered. For example, we consider a minimum of 0.01 h^{-1}, which gives us a response time of the order of 100 h. On the other extreme we considered 0.35 h^{-1}. This value yields a response time of the order of 3 h. For this interval and other parameters taken from Tables 1 and 5, Fig. 31 shows the bifurcation diagram of

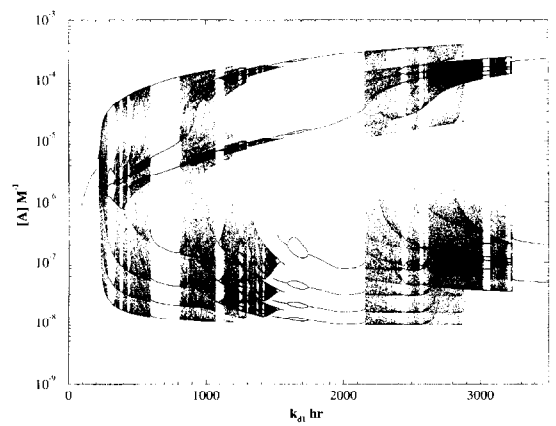

Fig. 24. Bifurcation diagram of [A] calculated using Poincaré sections of local maxima. Parameters were taken from Table 1 and Table 5 with $k_{rep} = 3.0\ h^{-1}$ and k_{d1}, the bifurcation parameter, varying from zero to 3500 h^{-1}.

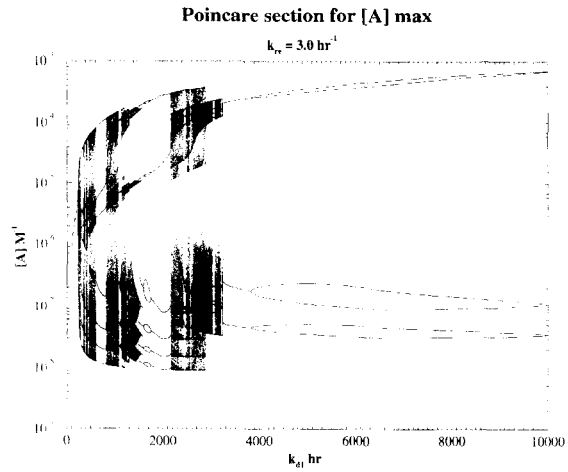

Fig. 25. Bifurcation diagram of [A] calculated using Poincaré sections of local maxima. Parameters were taken from Table 1 and Table 5, with $k_{rep} = 3.0\ h^{-1}$ and k_{d1}, the bifurcation parameter, varying from zero to 10000 h^{-1}.

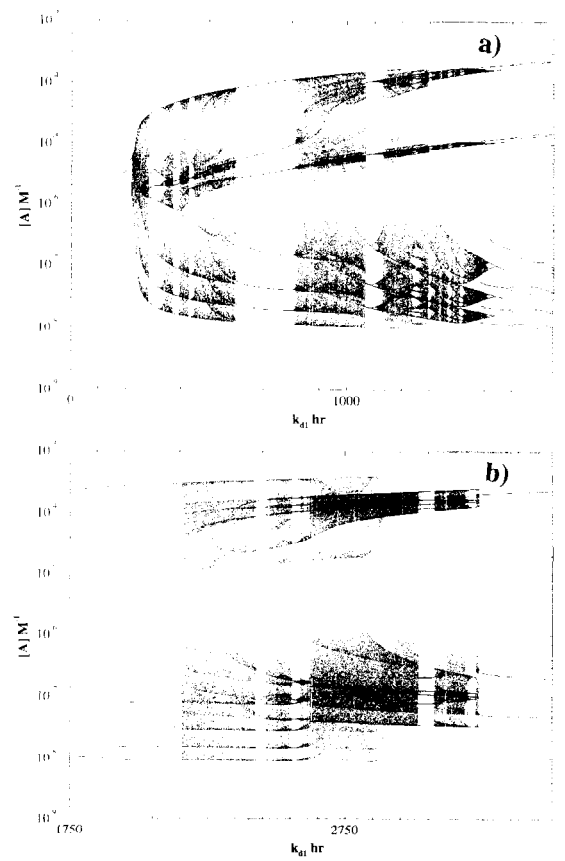

Fig. 26. Amplifications of Fig. 24: (a) k_{d1} h $\in$[0, 1750]; (b) k_{d1} h $\in$[1750, 2500].

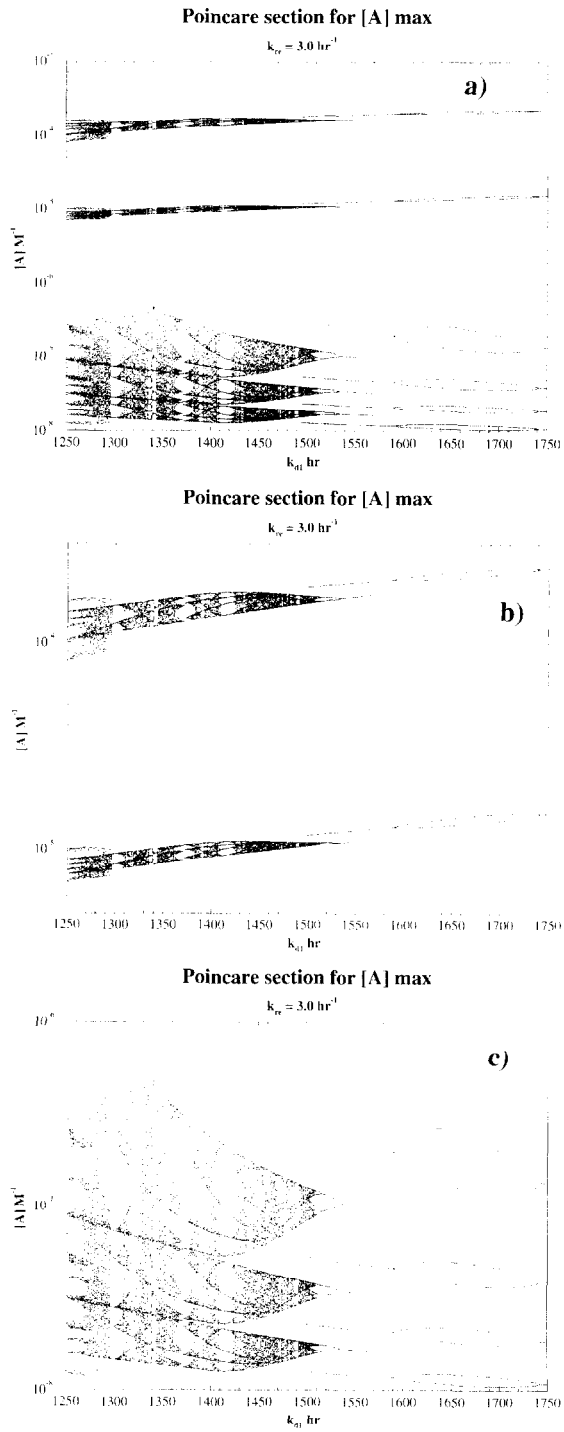

Fig. 27. Amplifications of Fig. 26 with k_{d1} h $\in$[1250, 1750]: (a) [A] $M^{-1} \in [10^{-8}, 10^{-3}]$; (b) A $M^{-1} \in [5\times10^{-6}, 3\times10^{-4}]$; (c) A $M^{-1} \in [10^{-8}, 10^{-6}]$.

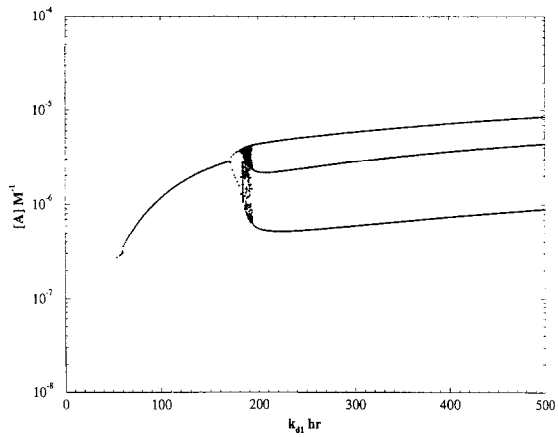

Fig. 28. Bifurcation diagram of [A] calculated using Poincaré sections of local maxima. Parameters were taken from Table 1 and Table 5, with $k_{rep} = 0.3$ h^{-1} and k_{d1}, the bifurcation parameter, varying from zero to 500 h^{-1}.

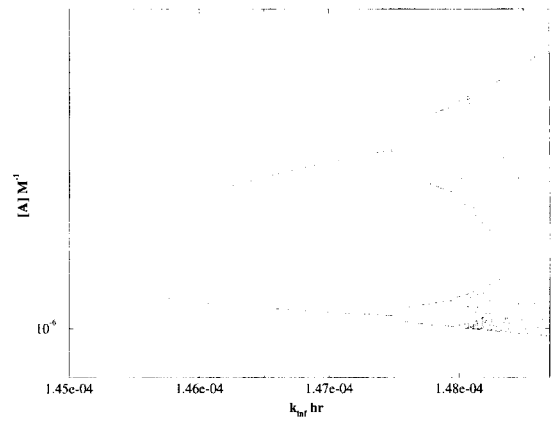

Fig. 30. Amplification of Fig. 29 depicting a period doubling route to chaos.

[Z], and Fig. 32 blows up the region between 0.10 and 0.20 h^{-1}. Notice interesting structures in the bifurcation diagram.

As a comparison we show in Fig. 33 the bifurcation diagram for [A], and Fig. 34 shows an amplification of the interval (0.034–0.044 h^{-1}) to show some of the bubble diagrams.

For k_0 we notice that, as the liver response time increases from approximately 3 h to 5 h, the system undergoes a period doubling route to chaos. For values of k_0 around 10 h we find more complex structures in the bifurcation diagram in the chaotic region, as can be seen in Figs. 32 and 33.

4.2.3. k_{rep}

The rate of reproduction, which is the only autocatalytic step in the mechanism, is readily estimated. For example, if we stretch the physical limits, we could consider a maximum value for k_{rep} of 10 h^{-1}. This value gives us roughly an average time between duplications of 6 min, which is unrealistically small. In bacteria and under optimal conditions, reproduc-

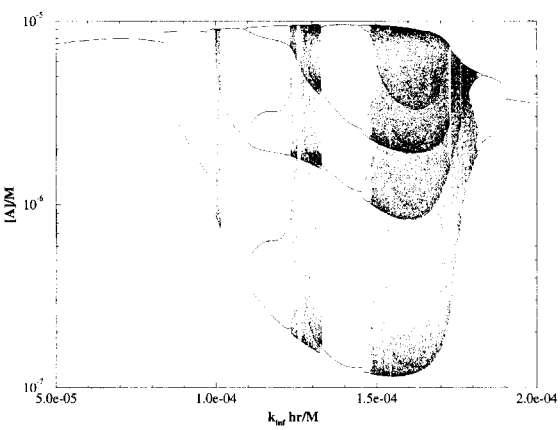

Fig. 29. Bifurcation diagram of [A] calculated using Poincaré sections of local maxima. Parameters were taken from Table 1 and Table 5, with k_{inf}, the bifurcation parameter, varying from 5×10^{-5} to 2×10^{-4}.

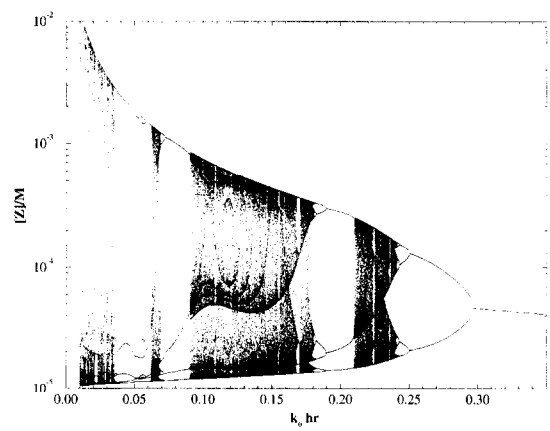

Fig. 31. Bifurcation diagram of [Z] calculated using Poincaré sections of local maxima. Parameters were taken from Table 1 and Table 5, with k_0, the bifurcation parameter, varying from zero to 0.35 h^{-1}.

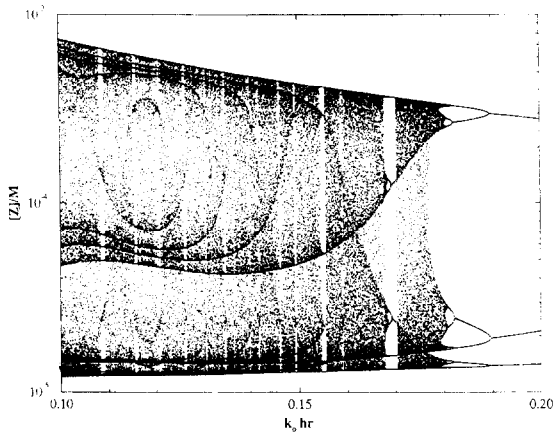

Fig. 32. Amplification of Fig. 31 with $k_0 \in [0.10, 0.20]$.

tion times are of the order of 20 min, or rates are of the order of 3.0 h^{-1}. On the other extreme, if we consider a value of k_{rep} of 0.001 h^{-1}, the replication time is of the order of 100 h. For this particular interval of k_{rep} values, we show in Figs. 35 and 36 the bifurcation diagrams for [Z] and [A]. Notice that, within the physical bounds considered in this work, a chaotic region exists.

4.2.4. k_{0A}

The final parameter considered in this analysis is k_{0A}. This parameter results from a contraction of several mechanistic steps. For this parameter we

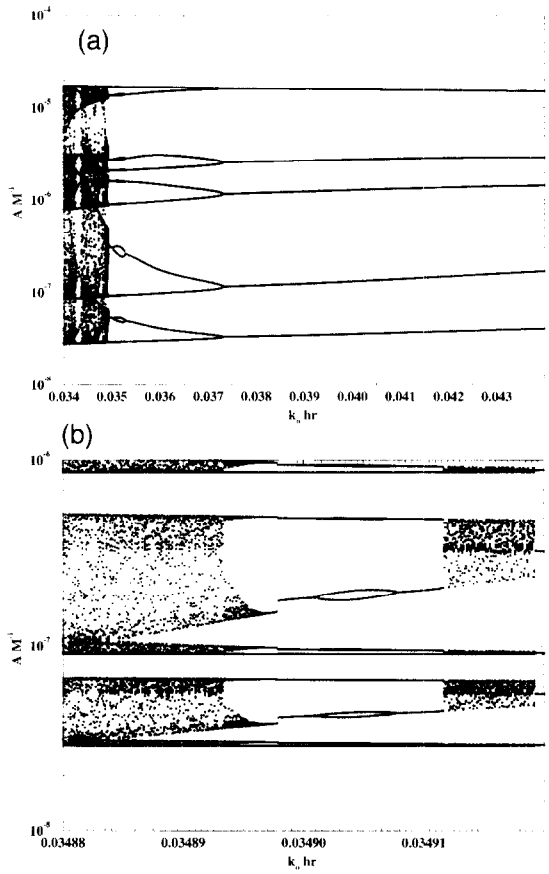

Fig. 34. Amplifications of Fig. 33 with (a) k_0 h $\in [0.034, 0.044]$ and [A] $M^{-1} \in [10^{-8}, 10^{-4}]$; (b) k_0 h $\in [0.03488, 0.03492]$ and [A] $M^{-1} \in [5 \times 10^{-8}, 3 \times 10^{-6}]$.

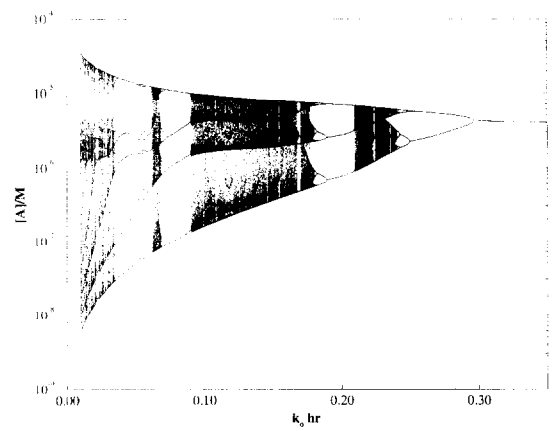

Fig. 33. Bifurcation diagram of [A] calculated using Poincaré sections of local maxima. Parameters were taken from Table 1 and Table 5, with k_0, the bifurcation parameter, varying from zero to 0.35 h^{-1}.

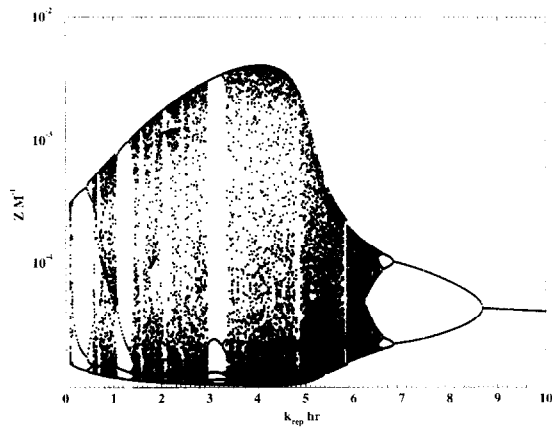

Fig. 35. Bifurcation diagram of [Z] calculated using Poincaré sections of local maxima. Parameters were taken from Table 1 and Table 5, with k_{rep}, the bifurcation parameter, varying from zero to 10 h^{-1}.

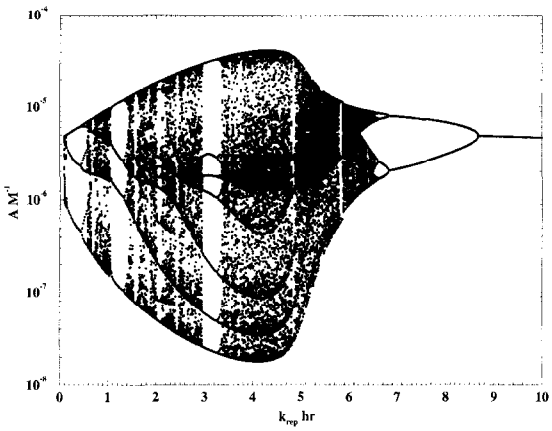

Fig. 36. Bifurcation diagram of [A] calculated using Poincaré sections of local maxima. Parameters were taken from Table 1 and Table 5, with k_{rep}, the bifurcation parameter, varying from zero to 10 h^{-1}.

considered values from 10^{10} to 10^{12} M^{-1} h^{-1}. Figs. 37 and 38(a) depict the bifurcation diagrams using a Poincare section for the maximum values of [Z] and [A]. We notice a small region around 10^{11} that shows chaos. In Fig. 38(b), we observe a period doubling route to chaos.

For the contraction done in the minimal model, the parameter interval considered in this work is reasonable and is consistent with an extended model of the alternative pathway of complement, which

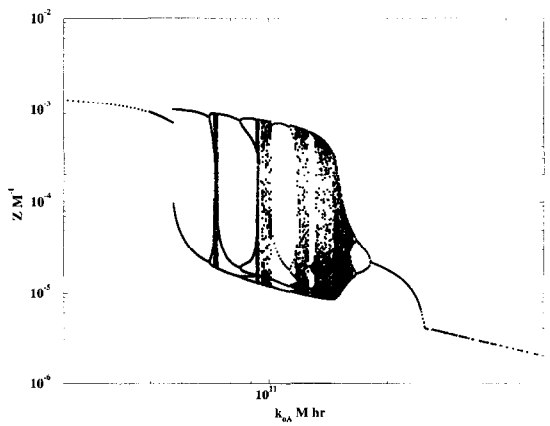

Fig. 37. Bifurcation diagram of [Z] calculated using Poincaré sections of local maxima. Parameters were taken from Table 1 and Table 5, with k_{0A}, the bifurcation parameter, varying from 3×10^{10} M^{-1} h^{-1} to 5×10^{11} M^{-1} h^{-1}.

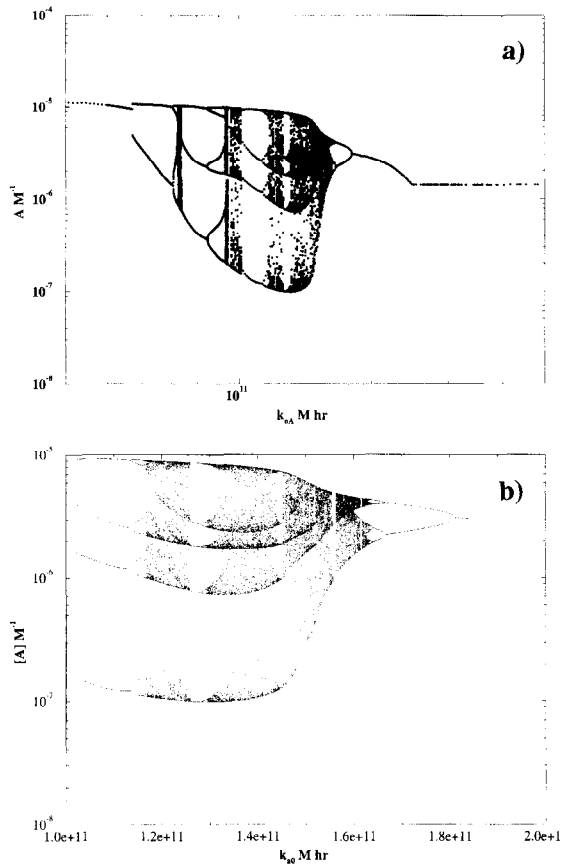

Fig. 38. Bifurcation diagram of [A] calculated using Poincaré sections of local minima. Parameters were taken from Table 1 and Table 5, with k_{0A}, the bifurcation parameter, varying from (a) 4×10^{10} M^{-1} h^{-1} to 5×10^{11} M^{-1} h^{-1}, and (b) 1.0×10^{11} M^{-1} h^{-1} to 2.0×10^{11} M^{-1} h^{-1}.

considers in more detail the C3 convertase attack of the cell membrane [27].

5. Conclusions

In the present work we have extended the analysis of the minimal model of the alternative pathway of the complement system. In particular, we have considered different values of the five parameters which can be related to deficiencies or pathological behavior. For these parameters we considered intervals of values within physical bounds. For these intervals, we found complex periodic oscillations and chaotic oscillations. Also, we constructed bifurcation dia-

grams using Poincaré sections of local maxima. These diagrams illustrate the complex oscillation intervals and the chaotic intervals in parameter space. Finally, the trends observed from this analysis seem reasonable and physically plausible. For example, when the replication constant decreases in value, which means that the half-life increases, the chaotic interval of k_{d1} shrinks. In the case of the external regulation of [A], if the response time decreases or k_0 increases, we observe a tendency to stable oscillations in the concentrations.

Acknowledgements

The authors gratefully acknowledge the support from NSF through grants CHE89-15945 and CHE93-12160. Also, one of us (E.P.-L.) has been partially supported by an NSF Research Opportunity Award during his sabbatical leave at the University of California Davis.

References

[1] H.C. Hemker and P.W. Hemker, General kinetics of enzyme cascades, Proc. R. Soc. London, B173 (1969) 411–420.
[2] S.K.A. Law and K.B.M. Reid, Complement, IRL Press, Oxford, 1988.
[3] P.B. Morgan, Complement: Clinical Aspects and Relevance to Disease, Academic Press, San Diego, CA, 1990.
[4] H. Müller-Eberhard, Molecular organization and function of the complement system, Annu. Rev. Biochem., 57 (1988) 321–347.
[5] M.P. Dierich, T.F. Schulz, A. Eigentler, H. Huemer and W. Schwäble, Structural and functional relationships among receptors and regulators of the complement system, Mol. Immunol., 25 (1988) 1043–1051.
[6] K.M. Pruitt, M.E. Turner and R.J. Boackle, A kinetic model for the quantitative analysis of the complement, J. Theor. Biol., 44 (1974) 207–217.
[7] E.W. Montroll, Enzymes cascades and their control in blood plasma, Adv. Chem. Phys., 26 (1974) 145–176.
[8] K.L. Queeney, A kinetic model of the alternative pathway of complement, B.A. Thesis, Williams College, 1992.
[9] K.L. Queeney and E. Peacock-López, Complex dynamics in a minimal model of the alternative pathway of the complement system, Biophys. Chem., 46 (1993) 101–115.
[10] T.S. Parker and L.O. Chua, Practical numerical algorithms for chaotic systems, Springer, New York, 1989.
[11] E. Juang and E. Peacock-López, Steady state approximatization in the minimal model of the alternative pathway of complement, Biophys. Chem., submitted.
[12] D.K. Kahaner and D.D. Barnett, Plotted solutions of differential equations (PLOD), Version 6.00, NIST, Washington, DC, 1989.
[13] H.T. Banks, Modeling and control in the biomedical sciences, Springer, Berlin, 1975.
[14] G.I. Marchuk, Mathematical Models in Immunology, Optimization Software, New York, 1983.
[15] C.W. Gear, The numerical integration of ordinary differential equations, Math. Comput., 21 (1967) 146.
[16] S. Levin (Ed.), Oscillations in Mathematical Biology, Springer, Berlin, 1983.
[17] T.A. Burton (Ed.), Modeling and Differential Equations in Biology, Marcel Dekker, New York, 1980.
[18] L.A. Segel (Ed.), Mathematical Models in Molecular and Cellular Biology, Cambridge University Press, Cambridge, 1980.
[19] G.W. Hoffmann and T. Hraba (Eds.), Immunology and Epidemiology, Springer, Berlin, 1986.
[20] R. Williams and W.R. Smith, Qualitative mathematical models of endocrine systems, Am. J. Phys., 245 (1983) R473–477.
[21] A. Kaczmarek and W.R. Adey, in H. Hanken (Ed.), Dynamics of Synergetic Systems, Springer Ser. Synergetics, Vol. 6, Springer, Berlin, 1980.
[22] M.L. Mackey and L. Glass, Science, 197 (1977) 287-289.
[23] L.F. Olsen and H. Degn, Q. Rev. Biophys., 18 (1985) 165.
[24] B. Hess and M. Markus, Trends. Biochem., 12 (1987) 45.
[25] H. Degn, A.V. Holden and L.F. Olsen (Eds.), Chaos in Biological Systems, NATO ASI Ser. A: Life Sciences, Vol. 138, Plenum Press, New York, 1987.
[26] B. Chance, E.K. Pye, A.K. Ghosh and B. Hess, Biological and Biochemical Oscillations, Academic Press, New York, 1973.
[27] E. Juang, Complex dynamics in the contracted and extended models of the alternative pathway of complement, B.A. Thesis, Williams College, 1995.